Efficient Calculation of Hydrodynamic Properties of OWC-Type Devices

D. V. Evans

R. Porter

School of Mathematics,
University of Bristol,
University Walk,
Bristol, BS8 1TW U.K.

A simple model of an OWC-type wave-energy device is used to illustrate a powerful accurate method for computing the hydrodynamic coefficients when sharp edges are present. The device consists simply of a vertical partially immersed circular cylinder open at either end, with power being extracted by constricting the flow of the air trapped in the cylinder above the internal free surface. The method involves the use of the theory of pressure distributions for OWC devices and the hydrodynamical coefficients are computed using an accurate Galerkin method which preserves the reciprocity relations.

1 Introduction

Mathematical modeling plays an important role in the design of efficient wave-energy devices and linear water-wave theory has proved extremely effective in predicting experimental results in moderate wave conditions. Early theoretical models relevant to devices such as the Salter duck or the Bristol submerged cylinder adapted existing ship hydrodynamic theory to include power take-off. Later, work of Falcão and Sarmento (1980), subsequently generalized by Evans (1982), addressed the modeling of OWC-type devices by considering the effect of a uniform pressure distribution over the free surface. Evans showed that hydrodynamical characteristics corresponding to added mass and radiation damping carried over to problems involving pressure distributions when the velocity of the rigid body and the exciting force on it when held fixed were replaced by the uniform free surface pressure imposed on the internal free surface and the induced volume flux across the free surface in the absence of a forcing pressure.

These new hydrodynamical characteristics, which Falnes has termed radiation conductance, corresponding to radiation damping, and radiation susceptance, corresponding to added mass, because of the analogy with electric circuit theory, play a key role in determining the overall efficiency or capture width as well as the bandwidth of a device. For this reason, it is essential to have efficient, accurate methods for determining these quantities, in particular where optimization of the device is being considered. Thus, Thomas and Ó Gallachóir (1993) have described an optimization procedure for the determination of the best choice of design parameters for a Bristol cylinder device in an appropriate incident wave spectrum and specified water depth. The method, which maximizes the sea efficiency for some allowable parameter range, is computationally intensive and depends on being able to compute the hydrodynamic properties rapidly and accurately. This is possible because a powerful multipole method is available for their computation because of the simplicity of the geometry of the Bristol cylinder. For asymmetric geometries such as the Salter duck, a general numerical approach is necessary, requiring many expensive evaluations of the appropriate Green function.

More recently, Evans et al. (1995) have used similar optimization techniques on a two-dimensional theoretical model of an OWC which correctly models the internal free surface (see Evans and Porter, 1995). The model consists of a two-dimensional vertical thin plate of arbitrary distance from a plane wall with a uniform pressure imposed on the free surface between the plate and the wall. Both the radiation problem and the scattering problem in the absence of the uniform pressure are considered. The technique involves expressing all the hydrodynamic characteristics in terms of the elements of a 2×2 real symmetric matrix whose elements are given by weighted integrals of the solutions of two singular integral equations with positive-definite kernels. A Galerkin method is used which accurately reflects the flow singularity at the edge of the plate and which enables the matrix to be determined extremely rapidly and accurately for all values of wave frequency and geometries. The method can also be applied to more general wave scattering problems involving two parallel partly immersed or submerged plates, as well as the OWC model (see Porter and Evans, 1995).

In this paper these ideas are extended to three dimensions. In Section 2, a brief summary of the theory of pressure distributions is given showing how the maximum efficiency or capture width ratio depends upon the hydrodynamical coefficients. The three-dimensional model chosen in Section 3 to illustrate the power of the method is a vertical thin-walled partly immersed rigid circular cylinder in a long-crested incident wave field. The scattering problem was first considered by Garrett (1970) in connection with floating harbors. Both the scattering problem and the corresponding radiation problem when the internal free surface is forced with a uniform pressure distribution are solved in a similar manner as for the two-dimensional problem, in this case expressing the hydrodynamic coefficients in terms of a 2×2 matrix related to weighted integrals of the solution of integral equations over the vertical cylindrical extension of the cylinder through the fluid depth. The power of the method will be illustrated by tables showing the rapid convergence of the results with increasing truncation parameter. It is also shown how various reciprocal relations are satisfied identically as part of the method of solution. Typical curves illustrating the hydrodynamical coefficients are presented including curves of the maximum capture width which can be achieved. Also shown are curves of the scattering cross section both with and without power absorption.

2 Theory of Pressure Distributions

For an oscillating-water-column wave-energy device, we expect the internal free surface of the device to be subjected to an oscillating pressure having the same frequency, ω, as the incident wave. In a rather complicated paper by Evans (1982), the general theory is constructed for the problem of an arbitrary number of such oscillating pressure distributions and the interactions between them with a view to wave-energy absorption

Contributed by the OMAE Division for publication in the JOURNAL OF OFFSHORE MECHANICS AND ARCTIC ENGINEERING. Manuscript received by the OMAE Division, July 1996; revised manuscript received, February 24, 1997. Associate Technical Editor: A. N. Williams.

from multiple OWC wave-energy devices. In this section, his theory is simplified for the case of just one device.

The device consists of walls enclosing an internal free surface (denoted by S_i) which is subjected to an oscillating pressure distribution of $p_a + P(t)$, where $P(t)$ has the same frequency, ω, as the incident wave and we assume that the horizontal pressure variation across S_i is negligible. There is a constant atmospheric pressure, p_a, above the external free surface, denoted by S_e. The water is assumed of constant depth h.

Under the assumptions of linear water-wave theory, there exists a velocity potential $\Phi(x, y, z, t)$, satisfying

$$\nabla^2\Phi = 0, \quad \text{in the fluid} \tag{1}$$

$$\Phi_n = 0, \quad \text{on solid boundaries} \tag{2}$$

where the suffix n denotes the normal derivative, while the linearized free surface condition becomes

$$g\zeta - \frac{\partial\Phi}{\partial t} = \begin{cases} (p_a + P(t))/\rho, & \text{on } S_i \\ p_a/\rho, & \text{on } S_e \end{cases} \tag{3}$$

where ρ is the density of the fluid and where $\zeta(x, z, t)$ is the surface elevation measured downwards and is related to the velocity potential through

$$\frac{\partial\zeta}{\partial t} = \frac{\partial\Phi}{\partial y}, \quad \text{on } y = 0 \tag{4}$$

It is assumed that the motion is time-harmonic with angular frequency ω and so we introduce the time-independent quantities ϕ, p, η by

$$\Phi(x, y, z, t) = \text{Re}\{\phi(x, y, z)e^{-i\omega t}\}$$
$$P(t) = \text{Re}\{pe^{-i\omega t}\},$$
$$\zeta(x, z, t) = \text{Re}\{\eta(x, z)e^{-i\omega t}\} \tag{5}$$

On combining (1)–(5), we find that the problem can now be expressed in terms of the time-independent velocity potential, ϕ, satisfying the following:

$$\nabla^2\phi = 0, \quad \text{in the fluid} \tag{6}$$

$$\phi_n = 0, \quad \text{on solid boundaries} \tag{7}$$

with

$$K\phi + \frac{\partial\phi}{\partial y} = \begin{cases} -i\omega p/\rho g, & \text{on } S_i \\ 0, & \text{on } S_e \end{cases} \tag{8}$$

where $K = \omega^2/g$. A suitable radiation condition must also be enforced.

Following the method of Evans (1982), we decompose the potential into two parts, such that

$$\phi = \phi^S - \frac{i\omega p}{\rho g}\phi^R \tag{9}$$

where ϕ^S is the potential associated with the scattering of an incident wave of unit amplitude from infinity in the absence of a pressure variation on S_i and satisfies (6)–(8) with $p = 0$. Here, ϕ^R is the potential describing the flow due to an oscillating pressure on S_i in the absence of an incident wave and satisfies (6), (7) with (8) replaced by

$$K\phi^R + \frac{\partial\phi^R}{\partial y} = \begin{cases} 1, & \text{on } S_i \\ 0, & \text{on } S_e \end{cases} \tag{10}$$

We call the boundary-value problem defined by (6), (7), and (10) the radiation problem.

We expect the amount of power that may be extracted by the device to depend on the induced volume flux across the internal free surface of the device, S_i. We call this quantity $Q(t)$ and the time dependence can be removed by writing $Q(t) = \text{Re}\{qe^{-i\omega t}\}$. Then, choosing positive flux as being measured vertically upwards, we have

$$q = -\int_{S_i}\frac{\partial\phi}{\partial y}\,dS = q^S - \frac{i\omega p}{\rho g}q^R, \quad \text{say,} \tag{11}$$

where q^S, q^R are the induced volume fluxes across S_i in the scattering and radiation problems, respectively, and are defined by

$$q^{S,R} = -\int_{S_i}\frac{\partial\phi^{S,R}}{\partial y}\,dS \tag{12}$$

Following Evans (1982), we make the convenient but arbitrary decomposition of the volume flux due to the radiation potential; thus

$$-\frac{i\omega p}{\rho g}q^R = -(\tilde{B} - i\tilde{A})p \tag{13}$$

where $\tilde{A}$ and $\tilde{B}$ are real and directly analogous to the added mass and radiation damping coefficients in a rigid-body system. By analogy with electric circuit theory, and following Falnes and McIver (1985), we shall call the complex quantity $\tilde{B} - i\tilde{A}$ the radiation admittance with $\tilde{B}$ the radiation conductance and $\tilde{A}$ the radiation susceptance. Clearly

$$\tilde{A} = -\frac{\omega}{\rho g}\text{Re}\{q^R\} \tag{14}$$

$$\tilde{B} = -\frac{\omega}{\rho g}\text{Im}\{q^R\} \tag{15}$$

The mean rate of working of the pressure force, or the mean power absorbed per unit area of the pressure distribution on S_i, W, is the time average of the pressure and the volume flux over a period of oscillation. This is just

$$W = \tfrac{1}{2}\text{Re}\{\bar{p}q\} = \tfrac{1}{2}\text{Re}\{\bar{p}q^S\} - \tfrac{1}{2}|p|^2\tilde{B}$$

from (11), (13)

$$= \frac{|q^S|^2}{8\tilde{B}} - \frac{\tilde{B}}{2}\left|p - \frac{q^S}{2\tilde{B}}\right|^2 \tag{16}$$

after rearranging, where the bar denotes the complex conjugate. This clearly takes a maximum value of

$$W_{\max} = \frac{|q^S|^2}{8\tilde{B}} \tag{17}$$

when

$$p = \frac{q^S}{2\tilde{B}} \tag{18}$$

The capture width l is defined to be the proportion of available power per unit crestlength of the incident wave which is extracted from the device. The maximum capture width is then

$$l_{\max} = \frac{W_{\max}}{P_w} \tag{19}$$

where P_w is the power per unit crestlength of the incident wave (that is, the mean energy flux per unit length across a vertical plane normal to the wave direction) and is given by

$$P_w = \rho g K k h/2\omega \tag{20}$$

when the incident wave is represented by $\phi_{\text{inc}}(x, y) =$

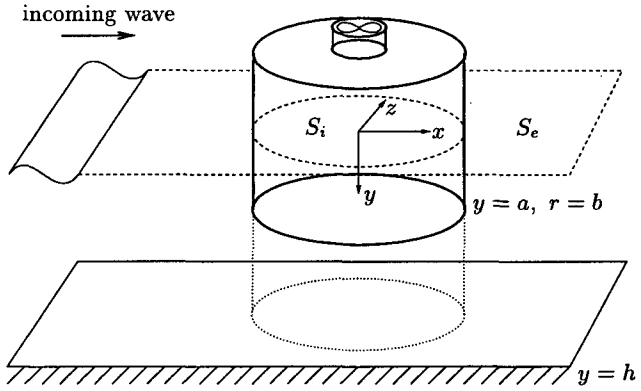

Fig. 1 Situation of the OWC duct device

$e^{\pm ikx}\psi_0(y)$. This maximum can only occur under the condition (18). In practice, it is difficult to control the pressure drop across the turbine, but it may be easier to control the volume flow rate across through the turbine. If we assume that these two quantities are related linearly and that the turbine characteristics do not allow a phase lag between the pressure and the volume flux to develop, then we may write

$$q = \Lambda p \tag{21}$$

where Λ is a real positive control parameter. Hence, $[\Lambda + (\tilde{B} - i\tilde{A})]p = q^S$; and so

$$W = \frac{|q^S|^2}{8\tilde{B}}\left\{1 - \frac{|\Lambda - (\tilde{B} + i\tilde{A})|^2}{|\Lambda + (\tilde{B} - i\tilde{A})|^2}\right\} \tag{22}$$

which takes a maximum value of

$$W_{\max} = \frac{|q^S|^2}{8\tilde{B}}\left\{1 - \frac{\Lambda_{\text{opt}} - \tilde{B}}{\Lambda_{\text{opt}} + \tilde{B}}\right\} \tag{23}$$

when $\Lambda = \Lambda_{\text{opt}}$ where

$$\Lambda_{\text{opt}} = (\tilde{B}^2 + \tilde{A}^2)^{1/2}. \tag{24}$$

The resulting maximum capture width is then given by

$$l_{\max} = \frac{|q^S|^2}{4P_w}\cdot\frac{1}{\Lambda_{\text{opt}} + \tilde{B}} \tag{25}$$

Details of the derivation of the foregoing theory can also be found in Evans (1982) or Smith (1983).

3 A Circular Duct OWC Device

Figure 1 shows the simple model of an oscillating-water-column wave-energy device being considered in this paper. The x and z axes are chosen to lie horizontally in the mean free surface with the y-axis vertically downwards with the seabed at $y = h$. A plane parallel-crested wave of unit amplitude traveling in the positive x direction is incident on the OWC device which consists of a thin open-ended circular cylinder, or duct, of radius b immersed to a depth a below the free surface, its center coinciding with the y-axis.

Cylindrical polars will be used and the time dependence is removed from the velocity potential by writing

$$\Phi(x, y, z, t) = \text{Re}\{\phi(r, \theta, y)e^{-i\omega t}\} \tag{26}$$

where we define

$$r = (x^2 + z^2)^{1/2}, \quad \text{and} \quad \theta = \tan^{-1}(z/x) \tag{27}$$

The potential, ϕ, is divided into radiation and scattering potentials, ϕ^S and ϕ^R, as in (9). A description of the boundary-value problems that these potentials must satisfy is given in Section 2 where the Laplacian operator in cylindrical coordinates is

$$\nabla^2 \equiv \frac{1}{r}\frac{\partial}{\partial r}\left(r\frac{\partial}{\partial r}\right) + \frac{1}{r^2}\frac{\partial^2}{\partial\theta^2} + \frac{\partial^2}{\partial y^2} \tag{28}$$

Applying a separation of variables procedure of the form $\phi(r, \theta, y) = \phi_n(r, \theta)\psi_n(y)$ to (6)–(8) (with $p = 0$), with (28) gives the depth eigenfunctions, $\psi_n(y)$, defined by

$$\psi_n(y) = N_n^{-1/2}\cos k_n(h - y), \quad n \geq 0 \tag{29}$$

with

$$N_n = \frac{1}{2}\left(1 + \frac{\sin 2k_nh}{2k_nh}\right), \quad n \geq 0 \tag{30}$$

where k_n, $n \geq 1$ are the positive real roots of

$$K + k_n \tan k_nh = 0 \tag{31}$$

while $k_0 = -ik$ and k is the positive real root of

$$K = k \tanh kh \tag{32}$$

and the wavelength is $\lambda = 2\pi/k$. In particular, we note that

$$\psi_0(y) = N_0^{-1/2}\cosh k(h - y),$$
$$N_0 = \frac{1}{2}\left(1 + \frac{\sinh 2kh}{2kh}\right) \tag{33}$$

Then ψ_n satisfy the following orthognality relation:

$$\frac{1}{h}\int_0^h \psi_n(y)\psi_m(y)dy = \delta_{mn} \tag{34}$$

Possible solutions for $\phi_n(r, \theta)$ which reflect the symmetry about the plane $z = 0$ are products of $\cos q\theta$, where q is an integer ≥ 0, and the Bessel functions J_q, H_q, I_q, and K_q where $H_q(x) \equiv H_q^{(1)}(x) = J_q(x) + iY_q(x)$ is the Hankel function of the first kind, chosen to ensure an outgoing potential when used in conjunction with (26).

In three-dimensional problems, the wave field away from the body may be written

$$\phi^R(x, y) \sim \mathcal{A}^R\left(\frac{2}{\pi kr}\right)^{1/2} e^{ikr - i\pi/4}\psi_0(y)$$

$$\phi^S(x, y) \sim \left[e^{ikx} + \mathcal{R}^S(\theta)\left(\frac{2}{\pi kr}\right)^{1/2} e^{ikr - i\pi/4}\right]\psi_0(y)$$

$$\text{as } r \to \infty \tag{35}$$

(see Mei, 1983, p. 307) where $\mathcal{A}^R$ and $\mathcal{R}^S(\theta)$ are defined to be radiation and scattering cross sections, respectively, the former constant due to the angular symmetry in the radiation problem.

Relations can be derived for this axisymmetric three-dimensional configuration using Green's second identity. Using the functions ϕ^R and ϕ^R in the identity leads to

$$\tilde{B} = \frac{\omega}{\rho g}4Kh|\mathcal{A}^R|^2 \tag{36}$$

while use of ϕ^S with ϕ^R gives, after use of the method of stationary phase

$$q^S = 4iKh\mathcal{A}^R \tag{37}$$

By combining (36) with (37) and using (20) to obtain

$$\tilde{B} = \frac{k|q^S|^2}{8P_w} \tag{38}$$

whence the maximum capture width defined by (25) becomes

$$l_{\max} = \frac{2\tilde{B}}{k(\Lambda_{\text{opt}} + \tilde{B})} \tag{39}$$

Note that if $\tilde{A} = 0$ at some frequency, we obtain the well-known point absorber result (e.g., Evans, 1976) $l_{\max} = k^{-1} = \lambda/2\pi$.

In what follows, the radiation and scattering problems are formulated in terms of functions related to the radial velocity across the gap under the circular duct, denoted by L_g, and the solution approximated using Galerkin's method.

3.1 The Radiation Problem. We divide the fluid domain into the two regions inside and outside the cylinder $r = b$. Using the set of possible solutions for $\phi_n(r, \theta)$, we construct general expansions satisfying all conditions of the problem apart from those on the cylinder $r = b$. Hence, in $r \geq b$, we write

$$\phi^R = \alpha_0^R H_0(kr)\psi_0(y) + \sum_{n=1}^{\infty} \alpha_n^R K_0(k_n r)\psi_n(y) \tag{40}$$

and in $r \leq b$

$$\phi^R = \beta_0^R J_0(kr)\psi_0(y) + \sum_{n=1}^{\infty} \beta_n^R I_0(k_n r)\psi_n(y) + K^{-1} \tag{41}$$

The term K^{-1} ensures that (10) is satisfied. We note that since the forcing of the internal free surface is independent of θ, there can be no angular variation in the potential, and so (40), (41) include only the $q = 0$ angular mode. We also note that, in the expansion for $r \geq b$, the first term represents the outgoing radiated wave, while the terms under the sum are all exponentially decaying modes. Defining $U^R(y)$ to be the outward radial velocity on $r = b$, we have

$$U^R(y) = \left.\frac{\partial \phi^R}{\partial r}\right|_{r=b}$$

$$= \alpha_0^R k H_0'(kb)\psi_0(y) + \sum_{n=1}^{\infty} \alpha_n^R k_n K_0'(k_n b)\psi_n(y) \tag{42}$$

$$= \beta_0^R k J_0'(kb)\psi_0(y) + \sum_{n=1}^{\infty} \beta_n^R k_n I_0'(k_n b)\psi_n(y) \tag{43}$$

$$= \sum_{n=0}^{\infty} U_n^R \psi_n(y), \quad \text{say} \tag{44}$$

and matching terms from (42) and (43) using (34) gives us

$$\alpha_0^R k H_0'(kb) = \beta_0^R k J_0'(kb)$$

$$= \frac{1}{h}\int_{L_g} U^R(y)\psi_0(y)dy = U_0^R \tag{45}$$

$$\alpha_n^R k_n K_0'(k_n b) = \beta_n^R k_n I_0'(k_n b)$$

$$= \frac{1}{h}\int_{L_g} U^R(y)\psi_n(y)dy = U_n^R \tag{46}$$

for $n \geq 1$, where $U^R(y) = 0$, $0 < y < a$ has been used. The continuity of ϕ across $r = b$, for $y \in L_g$ gives

$$0 = \alpha_0^R\left[H_0(kb) - \frac{H_0'(kb)}{J_0'(kb)} J_0(kb)\right]\psi_0(y) - K^{-1}$$

$$+ \sum_{n=1}^{\infty} U_n^R\left[\frac{K_0(k_n b)}{k_n K_0'(k_n b)} - \frac{I_0(k_n b)}{k_n I_0'(k_n b)}\right]\psi_n(y) \tag{47}$$

where (45), (46) have been used. Simplification of the foregoing equation can be achieved by employing the following Wronskian identities for Bessel functions (see Abramowitz and Stegun, 1964, Eqs. (9.1.16) and (9.6.15)):

$$J_n'(x)H_n(x) - H_n'(x)J_n(x) = -2i/\pi x \tag{48}$$

$$I_n'(x)K_n(x) - K_n'(x)I_n(x) = 1/x. \tag{49}$$

Thus, (47) becomes

$$\frac{-2i\alpha_0^R}{\pi kbJ_0'(kb)}\psi_0(y) - K^{-1}$$

$$+ \sum_{n=1}^{\infty} \frac{U_n^R}{k_n^2 b I_0'(k_n b)K_0'(k_n b)}\psi_n(y) = 0. \tag{50}$$

Hereafter, we will make use of the following relations for derivatives of Bessel functions:

$$\{H_0', J_0', K_0', I_0'\}(x) = \{-H_1, -J_1, -K_1, I_1\}(x).$$

Using these in the foregoing equation and substituting from (46) gives

$$\int_{L_g} U^R(t)L_0(y, t)dt = -K^{-1} + \frac{2i\alpha_0^R}{\pi kbJ_1(kb)}\psi_0(y), \quad y \in L_g \tag{51}$$

where the kernel is defined to be

$$L_0(y, t) = \sum_{n=1}^{\infty} \frac{\psi_n(y)\psi_n(t)}{k_n^2 hbI_1(k_n b)K_1(k_n b)} \tag{52}$$

We now introduce the functions $u_i(y)$ satisfying

$$\int_{L_g} u_i(t)L_0(y, t)dt = d_i(y), \quad y \in L_g, \quad i = 1, 2 \tag{53}$$

where

$$d_1(y) = 1, \quad \text{and} \quad d_2(y) = \psi_0(y) \tag{54}$$

Then, the combination

$$U^R(y) = -K^{-1}u_1(y) + \frac{2i\alpha_0^R}{\pi kbJ_1(kb)}u_2(y) \tag{55}$$

clearly satisfies (51). We also let the 2×2 matrix $\mathbf{S} = \{S_{ij}\}$ be defined by

$$S_{ij} = \int_{L_g} u_i(y)d_j(y)dy \tag{56}$$

We are interested in the induced volume flux, q^R and the far-field radiated wave amplitude $\mathcal{A}^R$. From (40), we note that, as $kr \to \infty$

$$\phi^R \sim \alpha_0^R H_0(kr)\psi_0(y) \sim \alpha_0^R\left(\frac{2}{\pi kr}\right)^{1/2} e^{ikr - i\pi/4}\psi_0(y) \tag{57}$$

so that, on comparison with (35), the far-field radiated wave amplitude is given by $\mathcal{A}^R = \alpha_0^R$. From (45)

$$-\alpha_0^R khH_1(kb) = \int_{L_g} U^R(y)\psi_0(y)dy$$

$$= -K^{-1}S_{12} + \frac{2i\alpha_0^R S_{22}}{\pi kbJ_1(kb)}, \tag{58}$$

and on rearrangement, we obtain

$$\mathcal{A}^R = \alpha_0^R = \frac{K^{-1}\pi kbJ_1(kb)S_{12}}{\gamma H_1(kb) + 2iS_{22}} \tag{59}$$

where $\gamma = \pi kbkhJ_1(kb)$ is real. The induced volume flux is given by

$$q^R = -\int_{S_i} \frac{\partial \phi^R}{\partial y}\, dS = -\int_{L_g}\int_0^{2\pi} U^R(y) b d\theta dy \qquad (60)$$

using continuity of flux arguments in $r < b$, $0 < y < h$. Substituting (55) into the foregoing and using (56) gives

$$q^R = -2\pi b\left[-K^{-1}S_{11} + \frac{2i\alpha_0^R S_{21}}{\pi kbJ_1(kb)}\right]$$

$$= \frac{2\pi K^{-1} b(\gamma H_1(kb)S_{11} + 2i\Delta)}{\gamma H_1(kb) + 2iS_{22}}, \qquad (61)$$

where $\Delta = S_{11}S_{22} - S_{12}S_{21}$.

Using this in (15) gives

$$\tilde{B} = \frac{\omega}{\rho g}\cdot\frac{4\pi K^{-1} b\gamma J_1(kb) S_{12}^2}{\gamma^2 J_1^2(kb) + (\gamma Y_1(kb) + 2S_{22})^2} \qquad (62)$$

It is a simple matter to show that the relation between $\mathcal{A}^R$ and $\tilde{B}$ given by (36) is in fact satisfied identically by comparison of (59) with (62). Previously, Thomas (1982), using a method of matched eigenfunction expansions, had used the relation (36) as a numerical check.

3.2 The Scattering Problem. In this section we consider the problem of the scattering of an incident wave traveling in the positive x direction in the absence of pressure variations on the internal free surface of the duct. We recall that the potential of the incident wave is given by $\phi_{\text{inc}} = e^{ikx}\psi_0(y)$. From Abramowitz and Stegun (1964, Eq. (9.1.41)), we have

$$e^{ikx} = \sum_{q=0}^{\infty} \epsilon_q i^q J_q(kr)\cos q\theta, \begin{cases} \epsilon_0 = 1, \\ \epsilon_q = 2, \quad q \geq 1 \end{cases} \qquad (63)$$

The presence of the incident wave destroys the angular symmetry enjoyed in the radiation problem and, as a result, the expansions for the scattering potential must include all $\cos q\theta$ modes. Bearing in mind the incident wave potential, the most general expansions for the scattering potential are, in $r \geq b$

$$\phi^S = \sum_{q=0}^{\infty} \epsilon_q i^q \cos q\theta[(J_q(kr) + \alpha_{q,0}^S H_q(kr))\psi_0(y) + \sum_{n=1}^{\infty} \alpha_{q,n}^S K_q(k_n r)\psi_n(y)] \qquad (64)$$

and in $r \leq b$

$$\phi^S = \sum_{q=0}^{\infty} \epsilon_q i^q \cos q\theta[\beta_{q,0}^S J_q(kr)\psi_0(y) + \sum_{n=1}^{\infty} \beta_{q,n}^S I_q(k_n r)\psi_n(y)] \qquad (65)$$

where it is noted that $\alpha_{q,0}^S$ are associated with the outgoing progressive waves, and $\beta_{q,0}^S$ represent the amplitudes of the standing wave modes inside the cylinder, whereas the terms under the sum over n are exponentially decaying disturbances.

We write

$$\phi^S = \sum_{q=0}^{\infty} \epsilon_q i^q \cos q\theta \chi_q^S(r, y) \qquad (66)$$

where $\chi_q^S(r, y)$ represents the terms in the square brackets in (64), (65) for $r \geq b$, $r \leq b$, respectively. Defining $U_q^S(y)$ to be the velocity across $r = b$ associated with the qth angular mode, we have

$$U_q^S(y) \equiv \left.\frac{\partial \chi_q^S}{\partial r}\right|_{r=b} = (kJ_q'(kb) + \alpha_{q,0}^S kH_q'(kb))\psi_0(y) + \sum_{n=1}^{\infty} \alpha_{q,n}^S k_n K_q'(k_n b)\psi_n(y)$$

$$= \beta_{q,0}^S kJ_q'(kb)\psi_0(y) + \sum_{n=1}^{\infty} \beta_{q,n}^S k_n I_q'(k_n b)\psi_n(y)$$

$$= \sum_{n=0}^{\infty} U_{q,n}^S \psi_n(y)$$

Multiplying the foregoing by $\psi_m(y)$ and integrating over $[0, h]$, gives

$$kJ_q'(kb) + \alpha_{q,0}^S kH_q'(kb) = \beta_{q,0}^S kJ_q'(kb) = \frac{1}{h}\int_{L_g} U_q^S(y)\psi_0(y)dy = U_{q,0}^S \qquad (67)$$

$$\alpha_{q,n}^S k_n K_q'(k_n b) = \beta_{q,n}^S k_n I_q'(k_n b) = \frac{1}{h}\int_{L_g} U_q^S(y)\psi_n(y)dy = U_{q,n}^S \qquad (68)$$

for $n \geq 1$, where we have used (34) and the fact that $U_q^S(y) = 0$ for $0 < y < a$. Continuity of the potential at $r = b$, $y \in L_g$ associated with the qth angular mode, gives from (64), (65)

$$0 = (J_q(kb) + \alpha_{q,0}^S H_q(kb) - \beta_{q,0}^S J_q(kb))\psi_0(y) + \sum_{n=1}^{\infty} (\alpha_{q,n}^S K_q(k_n b) - \beta_{q,n}^S I_q(k_n b))\psi_n(y)$$

$$= \frac{-2i\alpha_{q,0}^S}{\pi kbJ_q'(kb)}\psi_0(y) + \sum_{n=1}^{\infty} \frac{U_{q,n}^S}{k_n^2 bK_q'(k_n b)I_q'(k_n b)}\psi_n(y) \qquad (69)$$

where (67), (68) and the Wronskian identities for the Bessel functions have been used. Using (68) in the foregoing gives

$$\int_{L_g} U_q^S(t)L_q(y, t)dt = \frac{-2i\alpha_{q,0}^S}{\pi kbJ_q'(kb)}\psi_0(y), \quad y \in L_g, \qquad (70)$$

where

$$L_q(y, t) = -\sum_{n=1}^{\infty} \frac{\psi_n(y)\psi_n(t)}{k_n^2 hbI_q'(k_n b)K_q'(k_n b)} \qquad (71)$$

and $L_0(y, t)$ has already been defined in (52).

The induced volume flux across S_i, the internal free surface of the device is

$$q^S = -\int_{S_i} \frac{\partial \phi^S}{\partial y}\, dS = -\int_{L_g}\int_0^{2\pi} \left.\frac{\partial \phi^S}{\partial r}\right|_{r=b} b d\theta dy$$

$$= -b\sum_{q=0}^{\infty} \epsilon_q i^q \int_0^{2\pi}\int_{L_g} U_q^S(y)\cos q\theta dy d\theta$$

$$= -2\pi b\int_{L_g} U_0^S(y)dy \qquad (72)$$

where the first step comes from continuity of flux. Hence, the only contribution to q^S comes from the $q = 0$ mode as in the radiation problem of the previous section. This is expected due to the average of $\cos q\theta$ over S_i being zero for $q \neq 0$.

We notice that $U_0^S(y)$ satisfies (70) with $q = 0$, provided we define

$$U_0^S(y) = \frac{2i\alpha_{0,0}^S}{\pi kbJ_1(kb)}u_2(y) \qquad (73)$$

where $u_2(y)$ satisfies (53). Then, from (67) we have

$$-khJ_1(kb) - \alpha^S_{0,0}khHJ_1(kb) = \frac{2i\alpha^S_{0,0}}{\pi kbJ_1(kb)}\int_{L_g} u_2(y)\psi_0(y)dy$$

$$= \frac{2i\alpha^S_{0,0}}{\pi kbJ_1(kb)} S_{22} \tag{74}$$

where we have used (56). Rearranging gives

$$\alpha^S_{0,0} = \frac{-\gamma J_1(kb)}{\gamma H_1(kb) + 2iS_{22}} \tag{75}$$

with $\gamma = \pi kbkhJ_1(kb)$ as before. Also, from (72) we have

$$q^S = \frac{-4ib\alpha^S_{0,0}}{kbJ_1(kb)}\int_{L_g} u_2(y)dy = \frac{4\pi ikbhJ_1(kb)S_{21}}{\gamma H_1(kb) + 2iS_{22}} \tag{76}$$

Here, again it is clear that the relation (37) is satisfied identically on comparison of (76) and (59).

The far-field amplitude due to the scattering potential is given by

$$\phi^S \sim \sum_{q=0}^{\infty} \epsilon_q i^q \cos q\theta \alpha^S_{q,0} H_q(kr)\psi_0(y)$$

$$\sim \mathcal{R}^S(\theta)\left(\frac{2}{\pi kr}\right)^{1/2} e^{ikr - i\pi/4}\psi_0(y) \tag{77}$$

where

$$\mathcal{R}^S(\theta) = \sum_{q=0}^{\infty} \epsilon_q \alpha^S_{q,0} \cos q\theta \tag{78}$$

requires knowledge of the coefficients $\alpha^S_{q,0}$, for all q.

Returning to (70) and rescaling $U^S_q(y)$ by

$$U^S_q(y) = \frac{-2i\alpha^S_{q,0}}{\pi kbJ'_q(kb)} u^S_q(y) \tag{79}$$

shows that $u^S_q(y)$ satisfies

$$\int_{L_g} u^S_q(t)L_q(y, t)dt = \psi_0(y), \quad y \in L_g \tag{80}$$

with the kernel $L_q(y, t)$ defined by (71), while (67) becomes

$$khJ'_q(kb) + \alpha^S_{q,0}khH'_q(kb)$$

$$= \frac{-2i\alpha^S_{q,0}}{\pi kbJ'_q(kb)}\int_{L_g} u^S_q(y)\psi_0(y)dy \tag{81}$$

whence

$$\alpha^S_{q,0} = \frac{-\gamma_q J'_q(kb)}{\gamma_q H'_q(kb) + 2iA^S_q}, \tag{82}$$

where $\gamma_q = \pi kbkhJ'_q(kb)$ and

$$A^S_q = \int_{L_g} u^S_q(y)\psi_0(y)dy. \tag{83}$$

3.3 A Galerkin Approximation. In operator notation (53), (56) is written

$$\mathcal{L}_0 u_i = d_i, \quad y \in L_g, \quad i = 1, 2, \quad \text{with} \begin{cases} d_1 = 1, \\ d_2 = \psi_0 \end{cases} \tag{84}$$

$$(u_i, d_j) = S_{ij} \tag{85}$$

where $(\cdot, \cdot)$ denotes the inner product over the interval L_g. Once the matrix $\mathbf{S}$ has been found through a suitable approximation to u_i in (84), all the important properties of the problem are easily obtained. We approximate $u_i(y)$ by expanding in terms of a set of test functions, $\{v_n(y)\}$, which are defined later. Thus

$$u_i(y) \simeq \tilde{u}_i(y) = \sum_{n=0}^{N} a^{(i)}_n v_n(y), \quad i = 1, 2. \tag{86}$$

Substituting into (84), multiplying through by $v_m(y)$, $m = 0, \ldots, N$ and integrating over L_g gives

$$\sum_{n=0}^{N} a^{(i)}_n(v_m, \mathcal{L}_0 v_n) = (v_m, d_i), \quad m = 0, \ldots, N, \quad i = 1, 2, \tag{87}$$

or

$$\sum_{n=0}^{N} a^{(i)}_n L^{(0)}_{mn} = D^{(i)}_m, \tag{88}$$

where $L^{(0)}_{mn} = (v_m, \mathcal{L}_0 v_n)$ and $D^{(i)}_m = (v_m, d_i)$. Also, the approximation $\tilde{S}_{ij}$ to S_{ij} is

$$\tilde{S}_{ij} = \sum_{n=0}^{N} a^{(i)}_n(v_n, d_j) = \sum_{n=0}^{N} a^{(i)}_n D^{(j)}_n. \tag{89}$$

Now

$$L^{(0)}_{mn} = (v_m, \mathcal{L}_0 v_n) = \sum_{r=1}^{\infty} \frac{F_{mr}F_{nr}}{N_r k_r hk_r bI_1(k_r b)K_1(k_r b)}, \tag{90}$$

where (52) has been used, and $F_{mr} = (v_m, \psi_r)$. Analysis of the flow local to the lower edge of the duct would reveal a square-root singularity in the velocity of the fluid as the edge is approached. We incorporate this behavior into the set $\{v_m(y)\}$ by defining

$$v_m(y) = \frac{2(-1)^m}{\pi\{(h-a)^2 - (h-y)^2\}^{1/2}} T_{2m}\left(\frac{h-y}{h-a}\right),$$

$$a < y < h \tag{91}$$

as in Porter and Evans (1995, Eq. (2.43)), where $T_n(x) = \cos n\theta$, $x = \cos\theta$, is a Chebychev polynomial. This gives

$$F_{mr} = (v_m, \psi_r) = N_r^{-1/2} J_{2m}\{k_r(h-a)\} \tag{92}$$

For a detailed discussion on the choice of functions $\{v_m(y)\}$ see Porter and Evans (1995). From (90), we now have

$$L^{(0)}_{mn} = \sum_{r=1}^{\infty} \frac{J_{2m}\{k_r(h-a)\}J_{2n}\{k_r(h-a)\}}{N_r k_r hk_r bI_1(k_r b)K_1(k_r b)} \tag{93}$$

while

$$D^{(2)}_m = (v_m, d_2) = F(v_m, \psi_0)$$

$$= F_{m0} = (-1)^m N_0^{-1/2} I_{2m}\{k(h-a)\} \tag{94}$$

and

$$D^{(1)}_m = (v_m, 1) = \int_a^h \frac{2(-1)^m}{\pi\{(h-a)^2 - (h-y)^2\}^{1/2}}$$

$$\times T_{2m}\left(\frac{h-y}{h-a}\right)dy = \delta_{m0} \tag{95}$$

The approximation to the matrix $\mathbf{S}$ may now be computed from (89) once the coefficients $a^{(i)}_n$ have been found from (88). Alternatively, we may combine (88) and (89), giving the expression

$$\tilde{\mathbf{S}} = \mathbf{D}^T \mathbf{L}^{(0)^{-1}} \mathbf{D}, \tag{96}$$

where we have defined the $(N+1) \times (N+1)$ matrix $\mathbf{L}^{(0)} = \{L^{(0)}_{mn}\}$ and the $(N+1) \times 2$ matrix $\mathbf{D} = \{D_{mn}\}$, $D_{mn} = D^{(n)}_m$.

It is possible to show that the approximate values to the elements of the matrix $\mathbf{S}$ are in fact bounded in the foregoing in modulus by their true values. That is

$$|\tilde{S}_{ij}| \leq |S_{ij}|, \quad i, j = 1, 2 \tag{97}$$

A proof of this is given in Evans and Porter (1995).

We now turn our attention to approximating the far-field scattered amplitude which requires the knowledge of A_q^S, $q = 0, 1, 2, \ldots$. Equations (80) and (83) may be expressed in operator notation as

$$\left.\begin{aligned} \mathcal{L}_q u_q^S &= \psi_0, \quad y \in L_g, \\ (u_q^S, \psi_0) &= A_q^S, \end{aligned}\right\} \quad q = 0, 1, 2, \ldots \tag{98}$$

where u_q^S is unknown, and the kernel of the operator $\mathcal{L}_q$ is $L_q(y, t)$ and defined by (71). Performing a Galerkin approximation for each q along the lines of

$$u_q^S \simeq \tilde{u}_q^S = \sum_{n=0}^{N} b_n^{(q)} v_n(y) \tag{99}$$

with the set of test functions $\{v_n(y)\}$ defined by (91) and following the method outlined in the foregoing gives the approximation $\tilde{A}_q^S$ to A_q^S, written most simply as

$$\tilde{A}_q^S = \mathbf{F}^T \mathbf{L}^{(q)^{-1}} \mathbf{F} \tag{100}$$

where $\mathbf{F} = (F_{00}, \ldots, F_{N0})^T$ and F_{m0} is given by (94) and $\mathbf{L}^{(q)} = \{L_{mn}^{(q)}\}$ where

$$L_{mn}^{(q)} = -\sum_{r=1}^{\infty} \frac{J_{2m}\{k_r(h-a)\} J_{2n}\{k_r(h-a)\}}{N_r k_r h k_r b I_q'(k_r b) K_q'(k_r b)} \tag{101}$$

For a more detailed explanation of the foregoing procedure, see, for example, Porter and Evans (1995), where it is also shown that for such a system as occurs in (98), $0 < \tilde{A}_q^S \leq A_q^S$. The coefficients $\alpha_{q,0}^S$ are then found from (82) and the amplitude of the scattered wave field is given by (78).

4 Results

We introduce nondimensionalized quantities μ and ν to represent the radiation susceptance and radiation conductance coefficients through

$$\mu = \frac{\rho g}{\omega \pi b^2} \tilde{A} \tag{102}$$

and

$$\nu = \frac{\rho g}{\omega \pi b^2} \tilde{B} \tag{103}$$

so that the nondimensionalized maximum capture width ratio is given by

$$\frac{l_{\max}}{2b} = \frac{\nu}{kb((\nu^2 + \mu^2)^{1/2} + \nu)} \tag{104}$$

We choose to nondimensionalize the induced volume flux due to the scattering potential, $|q^S|$, by the volume flux across S_i due to a solid mass of fluid oscillating with the frequency and amplitude of the incident wave, $|q^I|$ say, giving rise to

$$\frac{|q^S|}{|q^I|} = \frac{N_0^{1/2} |q^S|}{\pi k b^2 \sinh kh} \tag{105}$$

These hydrodynamic coefficients are all expressible in terms of the elements of $\mathbf{S}$. The convergence of the Galerkin approximation to the elements of $\mathbf{S}$ is shown in Table 1. The estimates to S_{ij} for increasing values of truncation size, N, are all bounded in the foregoing by their true values and six-figure accuracy is attained for N as low as 3 in the chosen example. In all other cases, apart from a/h *very* small, choosing $N = 5$ assures six-figure accuracy in S_{ij} which translates into similar accuracy in the hydrodynamic coefficients. The infinite series defining the elements $L_{mn}^{(0)}$ are truncated at a value of $M = 1500$ for the figures in Table 1 and a leading order asymptotic correction similar to that described in Porter and Evans (1995) is used to improve accuracy of $L_{mn}^{(q)}$. For the figures that follow, $N = 5$, $M = 500$ is used.

Figures are presented each showing the variation of μ, ν and the modulus and phase of q^S with dimensionless parameter Kh for certain arrangements. Figures 2–3 are for a fixed submergence depth of $a/h = \frac{1}{2}$ and shows curves for b/h, the ratio of the duct radius to water depth, varying between $\frac{1}{8}$ and 1. The curves exhibit the behavioral patterns seen in the two-dimensional OWC model (see Evans and Porter, 1995). The large peaks in Figs. 2–3 are associated with the fundamental reso-

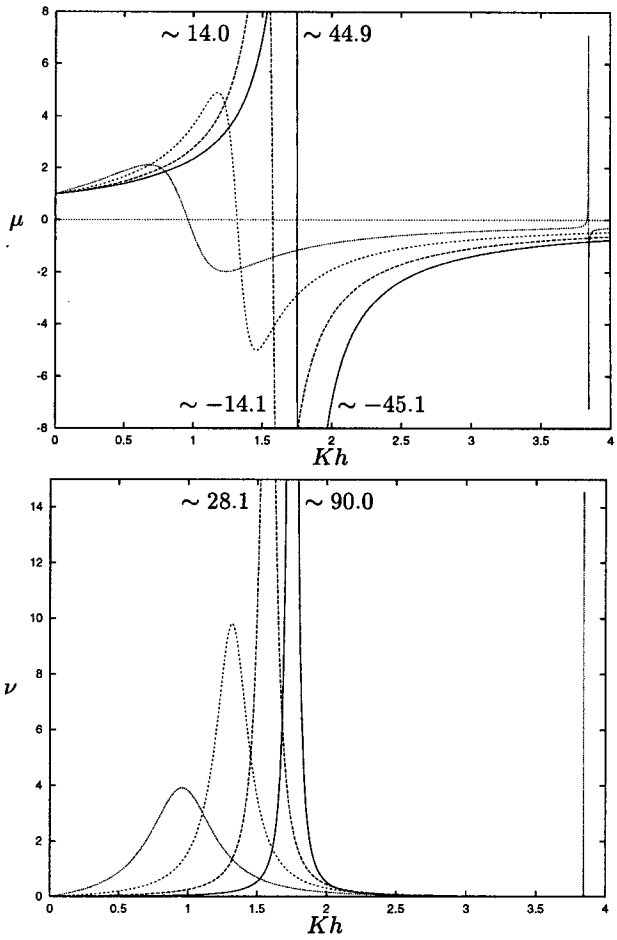

Fig. 2 The radiation susceptance (μ) and conductance (ν) coefficients against Kh in the case of $a/h = \frac{1}{2}$ for various duct radii: $b/h = \frac{1}{8}$(———), $\frac{1}{4}$(----), $\frac{1}{2}$(- - -), 1(· · · · · ·)

Table 1 Convergence of the elements of $\tilde{S}$, with increasing N in the case $a/H = \frac{1}{2}$, $b/h = \frac{1}{8}$, and $Kh = 1.7$

N	$\tilde{S}_{11}$	$\tilde{S}_{12} = \tilde{S}_{21}$	$\tilde{S}_{22}$
0	0.356038	0.248080	0.172856
1	0.407823	0.303642	0.232472
2	0.409336	0.305232	0.234144
3	0.409350	0.305247	0.234159
4	0.409350	0.305247	0.234159

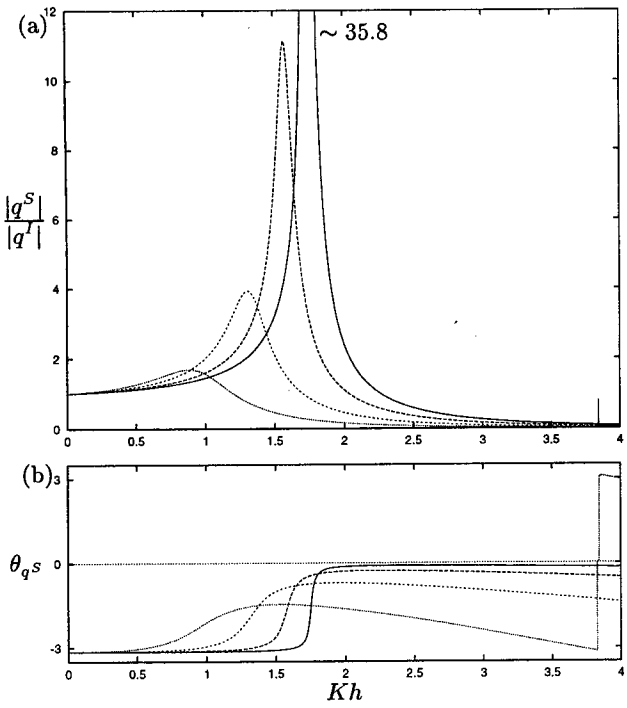

Fig. 3 The (*a*) magnitude and (*b*) phase of induced volume flux due to the scattering potential against *Kh* in the case $a/h = \frac{1}{2}$ for various duct radii: $b/h = \frac{1}{8}$(———), $\frac{1}{4}$(- - - -), $\frac{1}{2}$(- - -), 1(· · · · · ·)

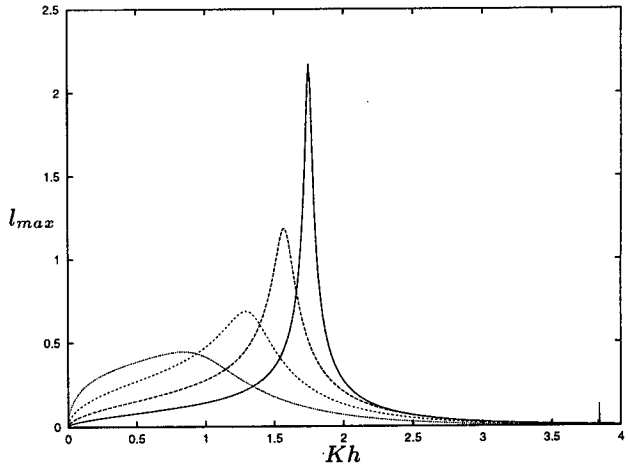

Fig. 4 The maximum capture width against *Kh* in the case of $a/h = \frac{1}{2}$ for various duct radii: $b/h = \frac{1}{8}$(———), $\frac{1}{4}$(- - - -), $\frac{1}{2}$(- - -), 1(· · · · · ·)

nance inside the duct. This resonance is associated with the approximate solid-body motion of the fluid in a narrow (b/a small) duct when excited by an incident wave, which, using simple hydrostatic arguments, is shown to occur at $Ka \approx 1$. Thus, we see that for a relatively narrow duct ($b/a = \frac{1}{4}$), the induced volume flux amplification factor, $|q^S/q^I|$, is very large (35.8). Notice that at resonance, the peak value of the radiation conductance is equal to the total variation from positive to negative in the radiation susceptance. An explanation for this in a related rigid body problem is given by Linton and Evans (1992).

At higher frequencies, further resonances occur each associated with the natural sloshing frequencies inside a duct whose walls extend throughout the depth. Resonances occur at zeros of $J_0'(kb)$ (or $J_1(kb)$) which are associated with the natural sloshing modes of fluid inside a vertical circular cylinder in finite depth. Note the first zero of $J_0'(kb)$ is at $kb = 3.831$. Garrett (1970) investigated these oscillations and also showed that large motions inside the duct due to an incident wave occur at values beyond these resonant frequencies, a phenomenon which we confirmed.

Figure 4 shows maximum capture width ratio computed from (104) using the accurately determined values of μ, ν as a function of Kh for various duct radii. Notice the characteristic increasing but narrowing peak as the radius is reduced with the resonance approaching the value $Ka \simeq 1$.

Finally, in Fig. 5, we show curves of the scattering cross section when a train of parallel-crested waves are incident on the partially immersed circular cylinder both when $p = 0$ (solid line) and at optimum power absorption (dotted line). This is presented diagramatically in the following way. The distance of a point P on the solid curve from the origin, O, represents the modulus of the scattering cross section in the direction θ, $|\mathcal{R}^S(\theta)|$, where θ is the angle between the line OP, and the positive x-axis and where the incident wave comes from $\theta = \pi$ (i.e., in the positive x direction). So, for example, in Fig. 5(b), the amplitude of the waves scattered "behind" the duct are large compared to those being reflected back in the direction of the oncoming waves.

The expression for $|\mathcal{R}^S(\theta)|$ in (78) is defined in terms of the coefficients $\alpha^S_{q,0}$, $q \geq 0$. Each $\alpha^S_{q,0}$ is related to A^S_q by (8) which is approximated by the lower bound $\tilde{A}^S_q$ in (100) as a

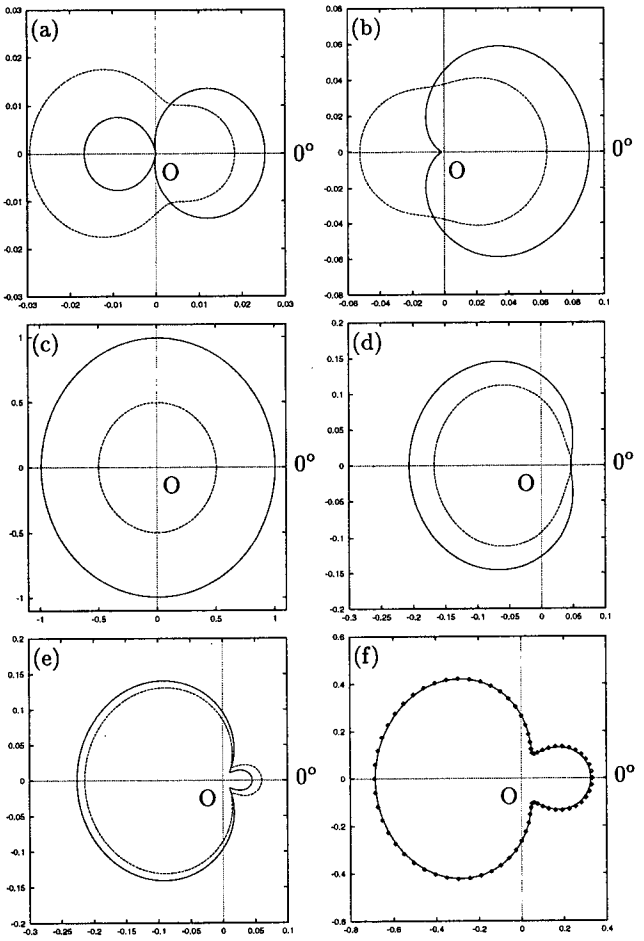

Fig. 5 $|\mathcal{R}^S(\theta)|$, the modulus of the scattered wave amplitude, measured from *O* as θ varies: $a/h = \frac{1}{2}$, $b/h = \frac{1}{8}$; (*a*) *Kh* = 1, (*b*) *Kh* = 1.5, (*c*) *Kh* = 1.75, (*d*) *Kh* = 2, (*e*) *Kh* = 2.5, (*f*) *Kh* = 5, ◇ are results for a cylinder extending to the bottom

result of a Galerkin approximation to the integral Eqs. (82), (83). The infinite series defining $|\mathcal{R}^S(\theta)|$ in (78) requires truncation for some value of q. Numerically, we find that $|\alpha^S_{q,0}|$ are rapidly decreasing coefficients as q increases and using the criterion $|\alpha^S_{q,0}| \leq 10^{-6}$ for truncation of the series, never more than 15 azimuthal modes are required. In most cases, only five modes are necessary for convergence.

In Figs. 5(*a*)–(*f*), we choose $a/h = \frac{1}{2}$, $b/h = \frac{1}{8}$ and vary Kh from 1 to 5. As Kh is increased, the influence of the gap under the duct becomes smaller and the scattering begins to resemble that of a vertical cylinder extending throughout the depth. The scattering of waves by such a geometry has a simple analytic solution (see Mei, 1983, p. 313) and the scattered wave amplitude is found to be

$$\mathcal{R}^S(\theta) = \sum_{q=0}^{\infty} \epsilon_q \frac{J'_q(kb)}{H'_q(kb)} \cos q\theta \qquad (106)$$

Figure 5(*f*) compares results for the duct with the full cylinder.

The dotted curves in each case show the scattering cross section when the device is tuned to absorb optimum power and are computed by combining the far-field radiated wave at optimum power absorption with $\mathcal{R}^S(\theta)$. Thus, from (35), (57), we compute

$$\left| \mathcal{R}^S(\theta) - \frac{i\omega p}{\rho g} \alpha^R_0 \right| \qquad (107)$$

where from (11), (13), (21), $p = q^S/(\Lambda_{\text{opt}} + \tilde{B} - i\tilde{A})$ with Λ_{opt} given by (24). It is not easy to draw general conclusions concerning the far field with and without power take-off. However, the difference in energy radiated from the duct with and without power take-off as a function of Kh attains a maximum at the resonant frequency. This can be seen in Fig. 5, where resonance occurs at $Kh = 1.75$ corresponding to curve (*c*). This is to be expected since the device will be taking optimum power from the sea at this frequency.

Conclusions

A variety of scattering cross sections can be achieved by varying the parameters of the problem and those in Fig. 5 are just typical of the variety of shapes which can occur. In all cases considered here, the power of the numerical technique has been confirmed and the method can be used with confidence to explore all global aspects of scattering by partially immersed ducts.

Figure 4 suggests that optimal capture widths will generally be very low and good device performance, corresponding to $l_{\max} > 1$, will only occur for relatively narrow ducts and very high volume fluxes. When compounded with the low efficiencies of existing power take-off mechanisms, these devices do not appear very attractive for long-term development as part of commercial wave-power plants.

The adaptation of the methods presented in this paper to a duct wave-energy device mounted on the seabed with a rigid-piston power take-off mechanism in the depths of the duct such as that considered by Simon (1981) is straightforward, as is the problem of scattering by a wholly immersed duct either mounted on the seabed or raised from the seabed using appropriate sets of functions introduced, as was done by Porter and Evans (1995) in considering the scattering of waves by different barrier configurations.

References

Abramowitz, M. A., and Stegun, I. 1964 *Handbook of Mathematical Functions,* Dover.

Evans, D. V., 1976, "A Theory for Wave-Power Absorption by Oscillating Bodies," *Journal of Fluid Mechanics,* Vol. 77, pp. 1–25.

Evans, D. V., 1982, "Wave-Power Absorption by Systems of Oscillating Surface Pressure Distributions," *Journal of Fluid Mechanics,* Vol. 114, pp. 481–499.

Evans, D. V., and Porter, R., 1995, "Hydrodynamic Characteristics of an Oscillating Water Column Device," *Applied Ocean Research,* Vol. 17, pp. 155–164.

Evans, D. V., Ó Gallachóir, B. F., Porter, R., and Thomas, G. P., 1996, "On the Optimal Design of an Oscillating Water Column Device," *Proceedings, 2nd European Wave Power Conference,* Lisbon, Portugal.

Falnes, J., and McIver, P., 1985, "Surface Wave Interactions With Systems of Oscillating Bodies and Pressure Distributions," *Applied Ocean Research,* Vol. 7(4), pp. 225–234.

Falcão, J., and Sarmento, A. J. N. A., 1980, "Wave Generation by a Periodic Surface Pressure and Its Application in Wave-Energy Extraction," 15th International Congress of Theoretical Applied Mechanics, Toronto, Ontario, Canada.

Garrett, C. J. R., 1970, "Bottomless Harbours," *Journal of Fluid Mechanics,* Vol. 43, pp. 433–449.

Linton, C. M., and Evans, D. V., 1992, "The Radiation and Scattering of Surface Waves by a Vertical Circular Cylinder in a Channel," *Phil. Transactions Royal Society London A* Vol. 338, pp. 325–357.

Mei, C. C., 1983, *The Applied Dynamics of Ocean Surface Waves,* Wiley Interscience, New York, NY.

Porter, R., and Evans, D. V., 1995, "Complementary Approximations to Wave Scattering by Vertical Barriers," *Journal of Fluid Mechanics,* Vol. 294, pp. 155–180.

Simon, M. J., 1981, "Wave-Energy Extraction by a Submerged Cylindrical Resonant Duct," *Journal of Fluid Mechanics,* Vol. 104, pp. 159–187.

Smith, C. M., 1983, "Some Problems in Linear Water Wave Theory," Ph.D. thesis, University of Bristol, Bristol, U.K.

Thomas, G. P., and Ó Gallachóir, B. F., 1993, "An Assessment of the Design Parameters for the Bristol Cylinder," *Proceedings, European Wave Power Symposium,* Edinburgh, Scotland, pp. 139–144.

Thomas, J. R., 1982, "The Hydrodynamics of Certain Wave Energy Absorbers," Ph.D. thesis, University of Bristol, Bristol, U.K.